A Recursive Calibration Approach for Smart Antenna Beamforming Frontend

Moh Chuan Tan[1, 2, a)], Minghui Li[1], Qammer H. Abbasi[1], Muhammad Imran[1]

[1] James Watt School of Engineering, University of Glasgow, Glasgow G12 8QQ, United Kingdom
[2] Research and Development Department, RFNet Technologies Pte Ltd, Singapore 319319
[a)] Corresponding author: tmohchuan@rfnetech.com

***Abstract* — In this work, a simple iteration-based approach is proposed for calibration and characterization of the frequency, phase and transmit power relationship in a smart antenna Radio Frequency (RF) beamforming frontend, which has a very low computational complexity. The RF frontend has been experimentally calibrated, and the beamforming results are verified with the 4 × 4 phase array. The RF frontend has been built using off-the-shelf components for easy realization. The proposed architecture with the closed-loop monitoring and control such as the power control (P*ctrl*), power detection (P*det)*, in addition to the phase control allows an automatic calibration of the beamforming weights, which forms a necessary process to ensure the accuracy of the antenna array beamforming.**

Index Terms—Beamforming, Phase error, Antenna Array, parameter compensation

I. INTRODUCTION

In the smart antenna industry, the Hybrid Beamforming (HBF) technique is one of the techniques that attracted many researchers due to its simplicity, cost-effectiveness and being able to achieve comparable results as compared to the digital beamforming. Hybrid beamforming combines both analog and digital beamforming components that are able to perform beamforming digitally and maintain the low cost. The hybrid beamforming architecture consists of a low-dimensional digital beamformer and a Radio Frequency (RF) beamformer implemented using the analog phase shifters, targeted to achieve low deployment cost and high scalability.

The advantages of the HBF system with a reduced number of RF chains have been presented in [1], where the energy efficiency (EE) and spectrum efficiency (SE) were evaluated on the reduced and optimum number of transceivers in the HBF system. The reduced number of RF chains for HBF in the wireless power transfer (WPT) system has been reported in [2]. The report has identified the optimum number of RF chains with respect to the number of antennas that is sufficient to achieve the fully digital beamforming performance, and also revealed that the software algorithm can be deployed, if the number of RF chains is not sufficient to support the large scale of antennas. In [3], the benefit of the HBF has been evaluated in an antenna system with a limited space and power consumption and the results revealed that the hybrid decoding offers a good compromise between the system performance and the power consumption.

In the beamforming process [4], both the amplitude and phase of each antenna element are controlled. A combined amplitude and phase control can be used to adjust the sidelobe levels and steer nulls more accurately as compared to the improvement by phase control alone. The combined relative amplitude $\mathbf{a_k}$ and phase shift $\boldsymbol{\phi_k}$ for each antenna is called a "complex weight" and is represented by a complex constant $\mathbf{w_k}$ (for the *kth* antenna). The complex weights $\mathbf{w_k}$ for the antenna elements are carefully chosen to give the desired peaks and nulls in the radiation pattern of the antenna array, the beamforming weight $\mathbf{w_k}$ is represented by the following equation [4]

$$w_k = a_k e^{j \sin(\emptyset_k)}$$
$$w_k = a_k \cos \emptyset_k + j a_k \sin \emptyset_k \quad (1)$$

Therefore, the precision of the amplitude and the phase of the RF beamforming frontend is extremely important to ensure the accuracy of the beam steering. The RF beamformer frontend shall be properly characterized and calibrated to offset the phase and amplitude error that was contributed by i) manufacturing tolerance such as PCB materials and process variations, ii) components tolerances, iii) performance variations due to frequency response and thermal effect, etc.

In [5], a phase optimization procedure based on the local search and the simulated annealing (SA) algorithm, taking into account the amplitude and phase errors of antenna element fields at every phase shift of the phase shifter is proposed to achieve more accurate beamforming of the phase array. A simple calibration procedure has been proposed in [6] to decrease the phase deviation during phase shift and gain control, the calibration results show that the phase error has been drastically mitigated.

In this work, we are focusing on the RF beamformer frontend that was designed to support a multiple linear phase array described in [7-8] in a HBF antenna system. The RF beamformer fronted was designed using the commercially available off-the-shelf components. A simple iteration-based method is proposed to calibrate the amplitude and phase error of the RF beamformer frontend. A customized RF beamformer

frontend has been developed instead of the off-the-shelf frontend which has limited control features that are important to realize the accuracy of the beamforming function, such as the wide dynamic gain control, high-resolution phase control, fast RF switching to support up to 4 antennas with the single chain and gain boost for transmitter and receiver.

This paper is organized as follows. In section II, we presented the proposed beamforming chain that is targeted to deploy in the hybrid beamforming antenna system, follow by section III, where the systematic approach to calibrate the phase and gain error offset, and the calibration results are presented as well as the beamforming results when integrated with the targeted antenna array. Section IV concludes the paper.

II. BEAMFORMING FRONTEND ARCHITECTURE

The block diagram of the RF beamforming chain reported in [9] is presented in Fig. 1. The RF beamforming frontend was designed to operate from 4.9 – 5.9 GHz. Each beamforming chain is designed to support an n × 4 antenna array, and only 4 sets of RF chains are needed to support 4 units of n × 4 arrays to form a 360° beamforming antenna system. Each RF beamforming chain consists of a fast switching single pole four throw (SP4T) with 4 ns switching speed for antenna switching, two single pole two throw (SPDT) switches to toggle between the transmit and receive paths, a 6 bits phase shifter with 5.625° resolution to vary the phase of each RF chain for antenna beam shaping, a low noise amplifier (LNA) for receiver and a power amplifier (PA) for transmitter which were added to boost the RF signal and compensate the insertion loss exhibited by the phase shifter, SP2T, SP4T, and power combiner. The RF attenuator (ATT) was populated to provide 30 dB dynamic transmit power range. The RF beamforming chain is controlled by an external peripheral via a microcontroller or a manual switch, for instance bit 0 to bit 5 transistor-transistor logic (TTL) for phase adjustment, analog voltage signal P*ctrl* to control the transmit power of the RF chain and the analog signal P*det* that can be used to monitor the transmit power generated by the PA.

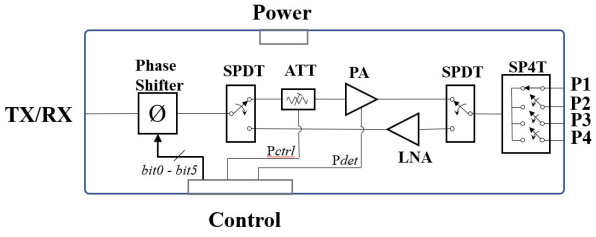

Fig. 1. Block Diagram of the RF Chain for n × 4 array

The RF beamformer chain is designed using the commercially available components mounted on a PCB which is fabricated using the industrial available materials such as RO4003 and FR-4. The key components used in the RF beamforming chain and their key specifications are listed in TABLE I. below.

TABLE I. KEY COMPONENTS SPECIFICATIONS

Parts	Part Number/ Maker	Key Specifications
Phase Shifter	HMC1133LP5E/ ADI	Phase Resolution: 5.625° Phase Coverage: 360°
RF Attenuator	IDTF2258NLGK/ IDT	Insertion Loss: 2.7 dB Attenuation Range: 33.6 dB
Power Amplifier	TQP5525/ Qorvo	Gain; 32 dB P1dB: 32 dBm
LNA	HMC717ALP3E/ ADI	Noise Figure: 1.3 dB Gain: 14.5 dB P1dB: 18 dBm
RF Switch (SP2T)	HMC8038LP4CETR/ ADI	Insertion loss: 1.3dB Ports Isolation: 51 dB
RF Switch (SP4T)	ADRF5044/ ADI	Insertion Loss: 1.7 dB Switching Speed: 4 ns Ports Isolation: 55 dB

The prototype of the beamforming frontend is presented in Fig. 2. The power and control of the RF beamformer chain are connected to the external power supply and the interface controller via the 6-way and 14-way cable assembly from Molex, PicoBlade series. The RF chain is powered by the multiple power supply +5V, +3.3V, -3.3V and -5V, which are separately driven by an external power supply. Multiple RF chains can be stacked up to form a beamforming chain to support multiple beamforming antenna arrays.

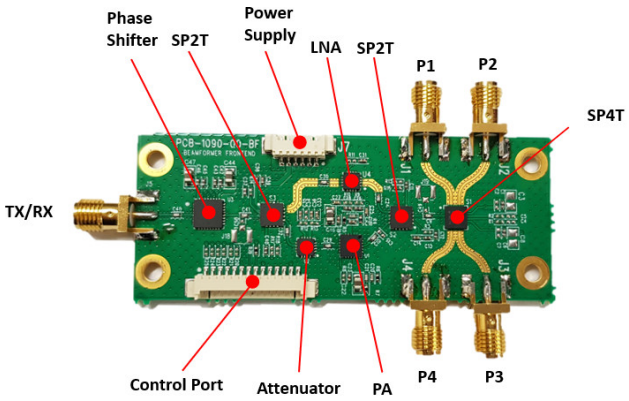

Fig. 2. The Prototype of the RF beamforming frontend

III. RF PARAMETERS CHARACTERIZATION

The calibration setup of the beamforming frontend is shown in Fig. 3, the phase shifter is controlled by the 6 bits TTL signal, the output power is control by adjusting the RF attenuator via the analog control signal P*ctrl* through an external power source, and the output power level is detected and converted to an analog voltage, P*det* that will be used to monitor the output power level during calibration. A Spectrum Analyzer (SA) and Vector Network Analyzer (VNA) is used to measure the transmit power and phase shift of the beamforming frontend. The equipment is connected to the individual port namely P1 to P4 to perform the calibration on the respective port.

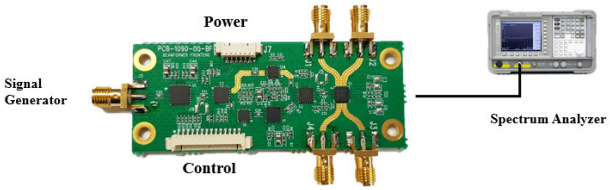

(a) Setup for transmitting power calibration

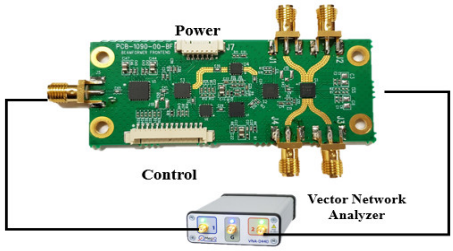

(a) Setup of phase calibration

Fig. 3. Calibration Setup

The transmit power response will be first characterized using the spectrum analyzer as shown in Fig. 3a, followed by the phase offset calibration using VNA as shown in Fig. 3b. The iteration flow involved in the calibration of the transmit power and phase is illustrated in Fig. 5. During the power detector P*det* calibration, the P*ctrl* voltage is adjusted between 0 V and 3 V, and the output power of the RF frontend and P*det* voltage is constantly measured, thus the relationship between P*ctrl*, P*det* and output power can be plotted, refer to Fig. 4. Once the P*det* characterization is done, the phase calibration can be carried out by controlling the P*ctrl* and monitoring the P*det* for constant power calibration, the phase error is observed by the VNA and iterated by controlling bit0 to bit5 of the phase shifter. The calibration process continues for other variables such as frequency, power, and repeats for Port 2, 3 and 4. The calibrated parameters are stored in the memory and will be used for self-compensation during the beamforming process.

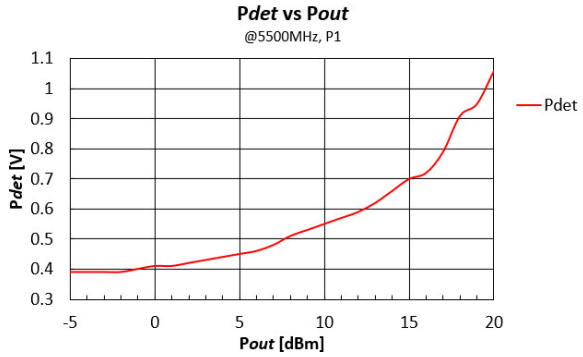

Fig. 4. Output Power and P*det*

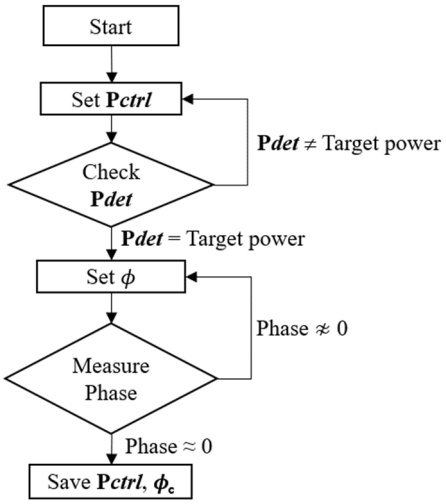

Fig. 5. Iteration flow for power and phase calibration

A. *Characterizing RF Output Power*

The power control of the RF chain is achieved by controlling the attenuator. The attenuation performance of the RF chain is shown in Fig. 6, the control voltage, P*ctrl* is ranged from 0.7 to 2.0 V, where 0.7 V gives 0 dB attenuation and the maximum attenuation of 30 dB occurs at 2.0 V.

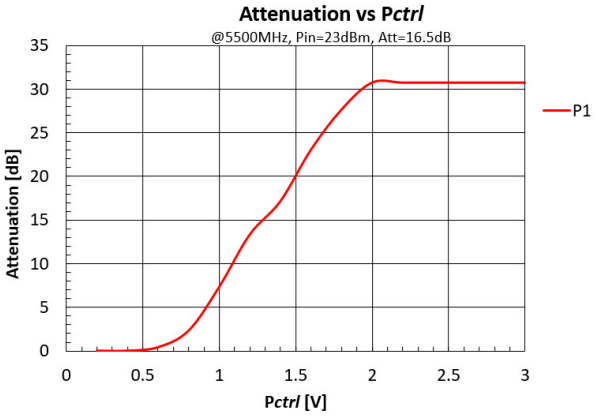

Fig. 6. Power Attenuation performance

In most of the cases, the output power of the RF chain varies according to the frequency and thermal response. The RF calibration will help to define the appropriate P*ctrl* to produce a flat transmit power response over the intended operating condition such as the frequencies and temperature. The frequency response chart for the transmit power is shown in Fig. 7, with P*ctrl* being at 0.8 V, the transmit output power tolerance as shown in the blue line is around +/2 dB over the frequency range from 5180 to 5880 MHz. The variation is probably due to the components and PCB manufacturing tolerances. The red line represents the transmit power after power calibration, the tolerance is improved to +/- 0.2 dB. The P*ctrl* voltage set to calibrate the transmit power is represented by the green line.

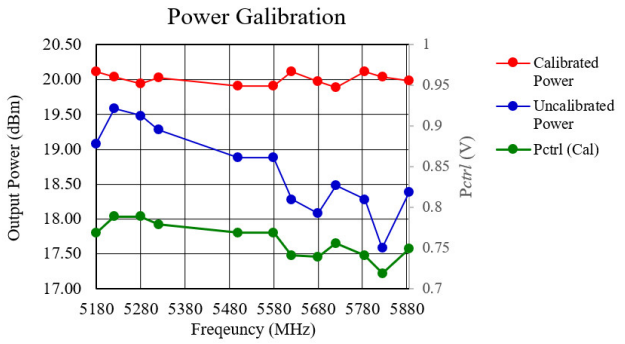

Fig. 7. Output Power Calibration

The gain flatness can be compensated automatically by initial calibration or calibration on-the-fly where the P*det* can be monitored regularly and the output power can be adjusted using the P*ctrl*, the automated adjustment procedure will make sure each of the RF chain to transmit at its desired power.

B. Characterizing Phase Error

The frequency response, manufacturing tolerance, and components tolerance are the major contributor to the phase tolerance in the RF chain. The phase tolerance must be properly identified and compensated to provide an accurate beam steering performance of the beamforming system. The phase error of the RF chain is measured using the VNA as described in Fig. 3b. The pre-calibration boards shown in the blue line has a phase difference of about 13° over the frequency band from 5180 to 5880 MHz. As mentioned earlier, the phase difference is contributed by several factors such as the manufacturing tolerance of the microstrip PCB, the phase error from the phase shifter, the frequency response, etc. The phase calibration result is shown in Fig. 8. The uncalibrated phase error is shown in the blue line, and the phase offset required to compensate the phase error is described by the orange line, ϕc. The red line represents the phase error after calibration with the phase error being improved to +/-1°.

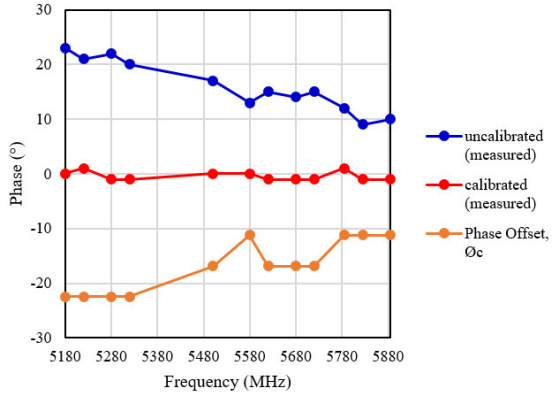

Fig. 8. Phase Calibration

C. Beam Steering Performance

The beamforming performance of the antenna array is measured by asserting the RF signal into each port of the antenna array with difference phase shift added by the phase offset ϕc calibrated earlier. The phase difference to each port is controlled by controlling the bit0 to bit5 of the 6-bits phase shifter. The phase difference for each port to enable 0°, + 40° and - 40° beam steering are presented in TABLE II. below, where ϕc_1, ϕc_2, ϕc_3, and ϕc_4 denote the calibrated offset value for each port.

TABLE II. PHASE COMPENSATION FOR BEAMFORMING CHAINS

	-40°	0°	+40°
Chain 1 (°)	ϕ_{c1}	ϕ_{c1}	45 + ϕ_{c1}
Chain 2 (°)	135 + ϕ_{c2}	ϕ_{c2}	270 + ϕ_{c2}
Chain 3 (°)	270 + ϕ_{c3}	ϕ_{c3}	135 + ϕ_{c3}
Chain 4 (°)	45 + ϕ_{c4}	ϕ_{c4}	ϕ_{c4}

The beamforming results evaluated with the compensated phase and chain power are presented in Fig. 9, where the beam steering angle agreed well with the simulated results. The compensated phase ϕ_c has successfully offset the phase difference between the RF chains. It was observed that the achievable beam steering resolution angle is around 2° by using the 6-bits phase shifter at each RF chain.

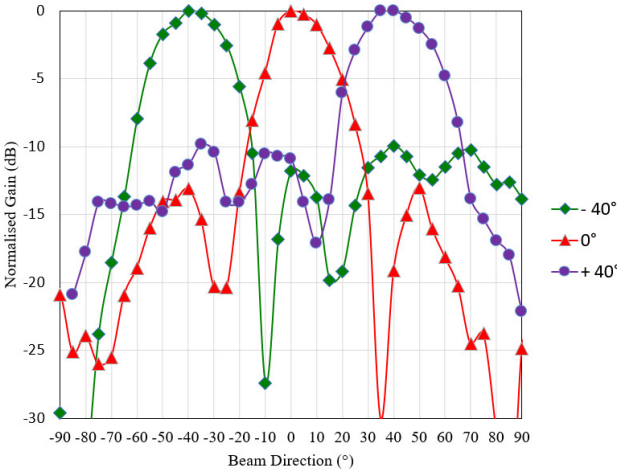

Fig. 9. Measured Beamforming Result with 4 × 4 array

IV. CONCLUSION AND FUTURE WORKS

An RF beamforming front end has been developed and characterized to support the generic phase antenna array for hybrid beamforming applications. A simple calibration method based on iterations has been deployed to calculate the phase and power compensation for the errors constituted by the manufacturing and components tolerance. The calibration results revealed that the necessary phase and power compensation are well-taken care, and the compensated values were further validated with the 4 × 4 linear antenna array.

As the future work, it would be interesting to deploy this iteration-based method to calibrate and compensate the power and phase offset with the presence of external factors such as temperature, humidity, and altitude, which may potentially affect the performance of the power and phase accuracy.

ACKNOWLEDGMENT

The authors would like to acknowledge and express sincere appreciation to the Singapore Economic Development Board (EDB) and RFNet Technologies Pte Ltd for financing and providing a good environment and facilities to support the project.

REFERENCES

[1] S. Han, et al., "Large scale antenna system with hybrid digital and analog beamforming structure," in *IEEE International Conference on Communications Workshops (ICC),* 2014, pp. 842-847.

[2] L. Yang, Y. Zeng, R. Zhang, "Wireless power transfer with hybrid beamforming: How many RF chains do we need?," in *IEEE Trans. Wireless Commun.*, 2018, vol. 17, no. 10, pp. 6972-6984.

[3] S. Ahmed, M. Sadek, A. Zekry, H. Elhennawy, "Hybrid analog and digital beamforming for space-constrained and energy-efficient massive MIMO wireless systems," in *Proc. 40th Int. Conf. Telecommun. Signal Process. (TSP), Barcelona, Spain*, Jul. 2017, pp. 186-189.

[4] T. Haynes, "A Primer on Digital Beamforming", in *Spectrum Signal Processing*, 1998.

[5] N. Nakamoto, T. Takahashi, Y. Konishi, I. Chiba, "Phase Optimization for Accurate Beam Forming of Phased Array with Element Field Errors at Every Phase Shift", in *IEEE International Symposium on Phased Array Systems and Technology*, 2013, pp. 693-697.

[6] Q. Fei, Y. Yu, X. Yin, L. Yang, Y. Lu, "Low-cost phase shifter and calibration solution for multi-channel receiver", in *IEEE International Conference on Ubiquitous Wireless Broadband (ICUWB)*, 2016, pp. 1-3.

[7] M. C. Tan, M. Li, Q. H. Abbasi, M. Imran, "A Wideband Beam forming Antenna Array for 802.11ac and 4.9 GHz", in *13th European Conference on Antenna and Propagation (EUCAP)*, 2019, pp. 1-3.

[8] M. C. Tan, M. Li, Q. H. Abbasi, M. Imran, "A Wideband Beamforming Antenna Array for 802.11ac and 4.9 GHz in Modern Transportation Market", to appear in *IEEE Transactions on Vehicular Technology*.

[9] M. C. Tan, M. Li, Q. H. Abbasi, M. Imran, "A Flexible Low-Cost Hybrid Beamforming Structure for Practical Beamforming Applications", in *IEEE International Symposium on Radio-Frequency Integration Technology (RFIT)*, 2019.